STAR FORMATION IN DISTANT RED GALAXIES: *SPITZER* OBSERVATIONS IN THE HUBBLE DEEP FIELD–SOUTH

Tracy M. A. Webb,[1] Pieter van Dokkum,[2,3] Eiichi Egami,[4] Giovanni Fazio,[5] Marijn Franx,[1] Eric Gawiser,[2,3,6] David Herrera,[2,3] Jiasheng Huang,[5] Ivo Labbé,[7] Paulina Lira,[6] Danilo Marchesini,[2,3] José Maza,[6] Ryan Quadri,[2] Gregory Rudnick,[8] and Paul van der Werf[1]

ABSTRACT

We present *Spitzer* 24 μm imaging of $1.5 < z < 2.5$ distant red galaxies (DRGs) in the $10' \times 10'$ extended Hubble Deep Field–South of the Multiwavelength Survey by Yale-Chile. We detect 65% of the DRGs with $K_{AB} < 23.2$ mag at $S_{24\,\mu m} \gtrsim 40$ μJy and conclude that the bulk of the DRG population is dusty active galaxies. A mid-infrared (MIR) color analysis with IRAC data suggests that the MIR fluxes are not dominated by buried AGNs, and we interpret the high detection rate as evidence for a high average star formation rate of $\langle \mathrm{SFR} \rangle = 130 \pm 30\ M_\odot\ \mathrm{yr}^{-1}$. From this, we infer that DRGs are important contributors to the cosmic star formation rate density at $z \sim 2$, at a level of $\sim 0.02\ M_\odot\ \mathrm{yr}^{-1}\ \mathrm{Mpc}^{-3}$ to our completeness limit of $K_{AB} = 22.9$ mag.

Subject headings: dust, extinction — galaxies: evolution — galaxies: high-redshift — galaxies: starburst — infrared: galaxies

1. INTRODUCTION

Through a variety of observational methods, we are building a census of the high-redshift universe and can now directly study galaxies in the process of forming. Color selection criteria effectively select large samples of galaxies at $z > 1$ such as Lyman break galaxies (LBGs; Steidel et al. 1999) and the massive distant red galaxies (DRGs; Franx et al. 2003). Selected by rest-frame optical colors to lie at $z \gtrsim 2$, DRGs exhibit properties of both passively evolved stellar populations and dusty starburst galaxies (Förster Schreiber et al. 2004; Labbé et al. 2005; Papovich et al. 2006). Characterizing this complex population and placing it into the context of the star formation history of the universe will elucidate our overall understanding of the assembly of massive galaxies.

Recent advances in the capabilities of infrared facilities have opened a new window onto the high-redshift universe. Through the direct detection of dust-enshrouded activity, mid-infrared (MIR) and far-infrared (FIR) studies provide orthogonal information to that gathered in the ultraviolet, optical, and near-infrared (NIR), which can be heavily biased by dust extinction. The work presented here addresses the nature of $z \sim 2$ DRGs through Multiband Photometer for *Spitzer* (MIPS) 24 μm and Infrared Array Camera (IRAC) imaging. We assume a $\Omega_M = 0.3$, $\Omega_\Lambda = 0.7$ cosmology and $H_0 = 70$ km s^{-1} Mpc^{-1} throughout.

[1] Leiden Observatory, University of Leiden, P.O. Box 9513, 2300 RA Leiden, Netherlands; webb@strw.leidenuniv.nl.
[2] Department of Astronomy, Yale University, P.O. Box 208101, New Haven, CT 06520-8101.
[3] Yale Center for Astronomy and Astrophysics, Yale University, P.O. Box 208121, New Haven, CT 06520.
[4] Steward Observatory, University of Arizona, 933 North Cherry Avenue, Tuscon, AZ 85721.
[5] Harvard-Smithsonian Center for Astrophysics, 60 Garden Street, Cambridge, MA 02138.
[6] Departamento de Astronomia, Universidad de Chile, Casilla, 36-D, Santiago, Chile.
[7] Observatories of the Carnegie Institute of Washington, 813 Santa Barbara Street, Pasadena, CA, 91101.
[8] National Optical Astronomy Observatory, 950 North Cherry Avenue, Tuscon, AZ 85719.

2. THE SAMPLE, *SPITZER* OBSERVATIONS, AND PHOTOMETRY

The DRG sample was drawn from the $10' \times 10'$ extended Hubble Deep Field–South (EHDF-S) of the Multiwavelength Survey by Yale-Chile (MUSYC; Gawiser et al. 2006). DRGs are defined by $(J - K)_{\mathrm{Vega}} > 2.3$ mag (Franx et al. 2003; van Dokkum et al. 2003), and, in this Letter, we focus on DRGs with $K_{AB} < 23.2$ mag (total magnitudes are given throughout), corresponding to the MUSYC 50% completeness limit (R. Quadri et al. 2006, in preparation).

Photometric redshifts were derived from *UBVRIz′JHK* photometry using the code presented in Rudnick et al. (2001, 2003), through linear combinations of galaxy templates, with an accuracy of $\langle |z_{\mathrm{spec}} - z_{\mathrm{phot}}|/(1 + z_{\mathrm{spec}}) \rangle = 0.05$ for $z > 1.5$. Here we have restricted our analysis to redshifts $1.5 < z < 2.5$ where the 6.2, 7.7, and 8.6 μm polycyclic aromatic hydrocarbon (PAH) features of star-forming galaxies fall into the *Spitzer* 24 μm filter. This provides a sample of 79 DRGs with a median redshift of $z = 2.0$.

The 24 μm observations were taken in the MIPS photometry mode and consist of six separate pointings. The central deepest pointing represents ~1 hr of frame time, and the five flanking pointings have 35 minutes of frame time each. The raw data were reduced and combined with the Data Analysis Tool developed by the MIPS instrument team (Gordon et al. 2005). The final image covers ~104 arcmin^2.

Imaging at 3.0, 4.5, 5.8, and 8.0 μm was taken in the IRAC mapping mode and mosaicked to produce a ~140 arcmin^2 image. Individual frames of 200 s were combined for a final total frame time, per location on the map, of 20 minutes. The *Spitzer* Science Center provides a Basic Calibrated Data product with flat-field corrections, dark subtraction, and linearity and flux calibrations. Additional steps conducted with the IRAC team customized software included pointing refinement, distortion correction, and mosaicking (Huang et al. 2004).

Photometry on the 24 μm image was performed using the point-spread function (PSF) fitting program DAOPHOT (Stetson 1987). The PSF was characterized using bright isolated point sources and then used to iteratively fit and subtract each object in the image. A small fraction (10/79) of DRGs were highly confused with neighboring objects, and these were removed from further analysis. We reached an average rms depth

of ~13 μJy and found the source counts to be in good agreement with Papovich et al. (2004). Because not all the DRGs are detected at 24 μm, their flux densities and upper limits were determined in a consistent manner by performing aperture photometry at each *K*-determined position after first subtracting all other objects in the catalog. We used 6″ diameter apertures and used the PSF stars to apply an aperture correction factor to total flux densities at 40″.

Due to the smaller beam size at the shorter IRAC wavelengths (<2″), and because highly confused DRGs have been removed from the sample, PSF fitting was not employed for the IRAC measurements. Aperture photometry (3″ diameter) was performed at the location of each DRG for each IRAC channel, again using isolated point sources to determine aperture corrections to total fluxes at 12.″2. The average rms depths are 2.6, 2.7, 4.3 and 4.0 μJy at 3.6, 4.5, 5.8, and 8.0 μm, respectively.

3. MIR CONSTRAINTS ON THE NATURE OF DRGs

At $1.5 < z < 2.5$, the 24 μm filter samples ~6–10 μm in the rest frame and the 24 μm flux offers a powerful method of differentiating between two basic spectral energy distribution (SED) types: active dusty galaxies, i.e., those that are powered by either star formation or active galactic nuclei (AGNs), both of which produce substantial mid-infrared emission, and passively evolved systems whose stellar flux drops drastically longward of ~2 μm (see Fig. 1). In pure starburst galaxies, the MIR emission is dominated by PAH features that are strong relative to the underlying dust continuum, which only begins to rise above ~10 μm. The hard radiation field of an AGN destroys PAH carriers, and the continuum emission from hot small dust grains is strong throughout the MIR (Genzel & Cesarsky 2000).

In Figure 1, we show the 24 μm flux densities for the DRGs, normalized to their rest-frame L_ν and overlaid with three template SEDs; 65% are detected at 24 μm, and the remainder are shown as 3 σ upper limits. This detection rate is in line with that found by Papovich et al. (2006) for DRGs in the Great Observatories Origins Deep Survey Chandra Deep Field–South, to a similar depth. All of the 24 μm–detected DRGs are incompatible with old stellar populations, and dusty starburst or AGN galaxies are required to produce such strong mid-IR emission. The sample shows a wide range in 24 μm flux, which we interpret primarily as a range in star formation rates. However, a real difference in PAH strengths, relative to the continuum, due to a range in metallicity or the hardness of the radiation field (e.g., Engelbracht et al. 2005; Hogg et al. 2005) could also be important, as could a variation in the level of AGN contamination of the MIR flux, although as we discuss below we deem this latter possibility unlikely.

The SEDs of DRGs that are not detected at 24 μm (35%) are consistent with passively evolved systems but also lower luminosity or less dusty starbursts, or starbursts that have weak or absent PAH signatures, as explained above. To investigate the nature of the 24 μm–faint DRGs, we used a stacking analysis to measure their mean 24 μm emission and find $S_{24\,\mu\mathrm{m}} = 10 \pm 2$ μJy. Thus, the remaining 35% of the sample cannot be entirely composed of passively evolved systems but contains some fraction of dusty starburst or AGN galaxies. A bootstrapping analysis indicates that this measurement is not dominated by a small number of systems, but beyond this we cannot constrain the fraction of starburst or AGN systems within this group.

Combining the 24 μm measurements with IRAC data provides

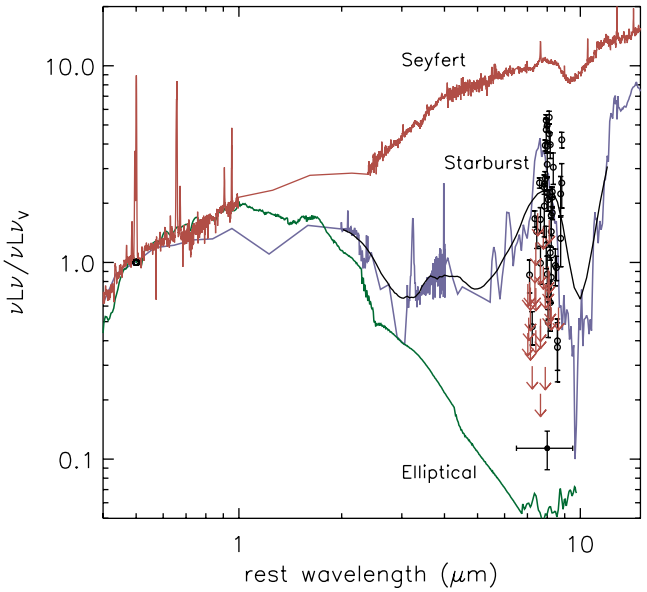

FIG. 1.—The 24 μm fluxes or limits of the DRGs, normalized to their rest-frame L_V. Circles are DRGs with 24 μm detections, and arrows show 3 σ upper limits for the remainder. The single filled circle below the arrows denotes the stacked measurement of DRGs that are not individually detected. Three SEDs are shown: the green line corresponds to an elliptical galaxy model (Coleman et al. 1980) extrapolated to longer wavelengths using *ISO* observations of local elliptical galaxies, the blue line to the observed SED of Arp 220, and the red line to the observed SED of NGC 1068 (J. Huang 2005, private communication). Because of the rapid variation in flux with wavelength for the Arp 220 SED in the MIR, we also show this SED smoothed by the 24 μm filter transmission curve (*solid black line*).

a color diagnostic of AGN activity (Fig. 2; Ivison et al. 2004; Egami et al. 2004; Huang et al. 2005). This technique relies on the different rest-frame NIR SED properties of AGN and starburst galaxies: stellar emission in starburst galaxies leads to a relatively flat SED in the rest-frame NIR, while hot dust around an AGN produces a power law that increases toward longer wavelengths. We have detected 50% of the 24 μm–bright DRGs at 4.5 and 8 μm, another 20% at 4.5 μm but not 8.0 μm, 5% in neither, and 25% fall off the IRAC channel 2/4 field of view. The colors (Fig. 2) indicate that star formation dominates the MIR emission of the DRGs, but as a conservative cut we consider the four objects with $S_{8\,\mu\mathrm{m}}/S_{4.5\,\mu\mathrm{m}} > 1.5$ to have *possible* AGN contamination. This is in agreement with results from the X-ray (Rubin et al. 2004; Reddy et al. 2005) and optical (van Dokkum et al. 2003), which also indicate that AGNs do not significantly contribute to the observed luminosity of DRGs. It should be remembered, however, that very heavily obscured or weak AGNs, although energetically unimportant in terms of observed MIR properties, may still be present.

4. STAR FORMATION RATES OF DRGs

PAH and MIR emission can be used to estimate the current star formation rate (SFR) of a galaxy (Wu et al. 2005). Using an Arp 220 SED template, we extrapolated from 24 μm/(1 + *z*) to rest-frame 6.75 μm. We then estimated L_{IR} through the 6.75 μm–F_{FIR} relation calibrated locally with the *Infrared Space Observatory* (*ISO*), which shows a scatter of ~50% (Elbaz et al. 2002). This value can then be converted to a SFR following the L_{IR}-SFR relationship of Kennicutt (1998) with an uncertainty of a factor of ~2–3. We note that adopting an M82-like SED instead

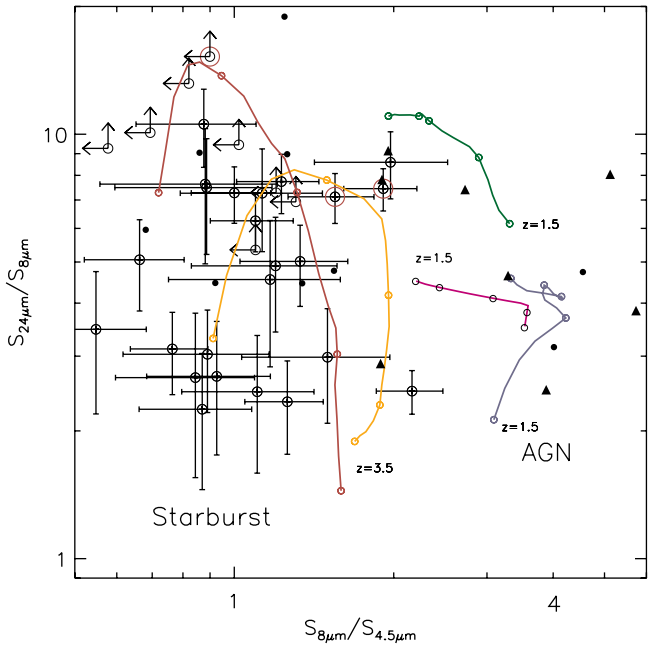

FIG. 2.—MIR color-color plot. The tracks correspond to two starburst SEDs (*leftmost*, *orange*: Arp 220; *red*: M82) and three AGN-dominated SEDs (*rightmost*, *magenta*: Mrk 231; *purple*: Seyfert 1 NGC 5506; *green*: Seyfert 2 NGC 1068). The SED tracks begin at $z = 1.5$ and are marked by circles in $z = 0.5$ steps, to $z = 3.5$. The open circles show DRGs from this work that are detected at 24 μm, with the radio-detected objects indicated by the large red circles. Also shown are *Spitzer* observed submillimeter-selected galaxies (*filled circles*; Egami et al. 2004) and optically faint AGNs (*filled triangles*; Rigby et al. 2005).

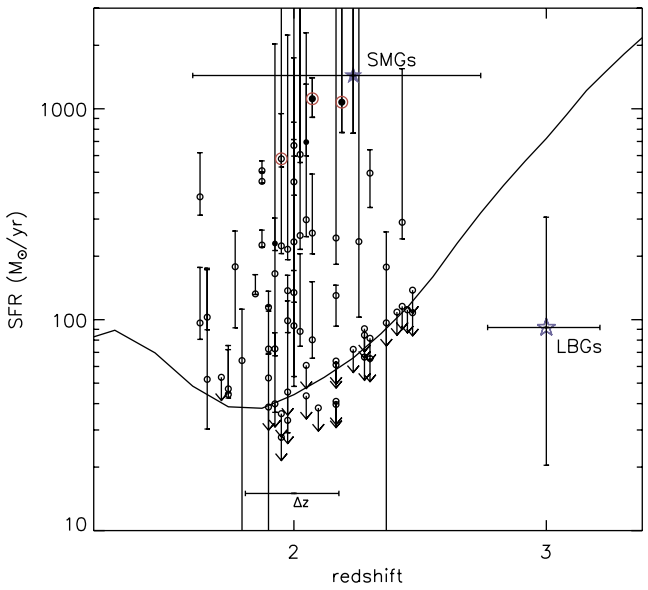

FIG. 3.—SFRs for DRGs as a function of redshift (*circles*). Filled circles mark DRGs that may contain AGNs, and red circles mark radio-detected galaxies. The solid line corresponds to the average effective SFR depth as a function of redshift, for these data. Also shown for reference is the median SFR for radio-detected submillimeter galaxies (SMGs) from Chapman et al. (2005; *filled star*) and that of LBGs from Shapley et al. (2001; *open star*).

of Arp 220 in the first step results in SFR estimates that are systematically 1.4 times lower.

In Figure 3, we plot the 24 μm SFRs or upper limits of the individual DRGs with redshift. The population is not homogeneous, and individual galaxies range in SFR from <30 to ~1000 $M_\odot$ yr^{-1}. A strong AGN contribution to the MIR flux will contaminate this estimate, by boosting the inferred SFR, and sources that may contain AGNs are marked. Also highlighted are three DRGs that are detected in the deep radio map of Huynh et al. (2005), two of which are possible AGNs based on their MIR colors. Studies indicate that the fraction of AGN contamination in the microjansky radio population increases at higher redshift (Richards 2000; Garrett 2001), and thus, the radio-detected DRGs may indeed contain weak AGNs. However, we note that these systems fall within 1 σ of the FIR/radio flux correlation of Condon (1992; with no systematic offset), which only holds for starburst galaxies, and thus significant AGN contamination is unlikely.

Using a stacking analysis, we calculated an average SFR for the entire DRG sample of $\langle \mathrm{SFR} \rangle = 130 \pm 30\ M_\odot$ yr^{-1}. This is the uncertainty-weighted mean of *all* 69 DRGs, when we assume no AGN contamination and a mean redshift of $z = 2$, with the uncertainty in the mean estimated from a bootstrapping analysis. This result is in good agreement with the optical SED modeling results of Förster Schreiber et al. (2004) of 120 $M_\odot$ yr^{-1}, and X-ray and submillimeter stacking analyses that estimate ~100–200 and ~100 $M_\odot$ yr^{-1}, respectively (Rubin et al. 2004; Reddy et al. 2005; Knudsen et al. 2005).

A significant source of error in this calculation is the photometric redshift uncertainty, since the rest-frame flux of starburst galaxies changes rapidly with wavelength in the region surrounding the PAH features. This effect was quantified by recalculating SFRs for simulated redshifts within Gaussian confidence intervals, and the resulting uncertainties are shown in Figure 3. The uncertainties are substantial, ranging from a factor of 2 to almost an order of magnitude.

We calculated the optically normalized SFRs (SFR/L_V) for the DRGs, which provide an indication of their age and/or dust content. We find $\langle \mathrm{SFR}/L_V \rangle \sim 19$[9], which is in excellent agreement with the submillimeter study of DRGs by Knudsen et al. (2005), who measure $\langle \mathrm{SFR}/L_V \rangle \sim 20$. However, the values for the DRGs show large scatter, ranging from $\mathrm{SFR}/L_V < 5$ to 200. Monte Carlo simulations indicate that the redshift uncertainties cannot account for the full range of this scatter and, moreover, the three radio-detected galaxies have the highest SFR/L_V, for a given L_V; as their radio flux confirms that they are extreme systems, their high SFR/L_V values are unlikely to stem solely from redshift uncertainties.

5. CONTRIBUTION TO THE COSMIC STAR FORMATION DENSITY

Using the 24 μm SFR estimates presented here, and the number density of DRGs in the MUSYC fields (known to a factor of 2; R. Quadri et al. 2006, in preparation), we estimate a star formation rate density (SFRD) for the DRGs of ~0.02 $M_\odot$ yr^{-1} Mpc^{-1} over the redshift range $1.5 < z < 2.5$ and to a depth of $K_{\mathrm{AB}} = 22.9$ mag. At this depth, our sample is 100% complete and therefore requires no completeness correction. A number of uncertainties affect this estimate, including those described in the previous sections: errors in the photometric redshifts, the uncertain conversion of an observed 24 μm flux to a SFR, and the potential contamination from AGNs. Also important are possible differences in dust properties and the initial mass function from low to high redshift, which are difficult to quantify. Nevertheless, although the uncertainties in

[9] In units of $M_\odot$ yr^{-1}($L_\odot \times 10^{-10}$)$^{-1}$.

the individual SFRs are high, the average SFR of the population is known to better accuracy since the redshift uncertainties, at least, are largely statistical.

The total SFRD, integrated over all galaxies, provides a census of the star formation history of the universe, and the relative contributions of different galaxy populations is indicative of their importance in assembling stellar mass. In a general sense, there is now reasonable agreement between IR and optical SFRD estimates at $z \sim 2$. Reddy et al. (2005) estimate a SFRD (from X-ray measurements) of 0.10 $M_\odot$ yr^{-1} Mpc^{-3} over $1.4 < z < 2.6$, for optical and NIR-selected galaxies, with DRGs producing 20% of this total. Likewise, Chapman et al. (2005) estimate ~0.1 $M_\odot$ yr^{-1} Mpc^{-3} for submillimeter-selected systems, after extending the submillimeter luminosity function down to $S_{850\,\mu\mathrm{m}} = 1$ mJy and applying a correction for AGN contamination. Thus, the two techniques converge on a similar value, and if we assume the $S_{850\,\mu\mathrm{m}} \sim 1$ mJy population encompasses the bulk of the optical and NIR-selected galaxies, and vice versa, this can be taken as a total SFRD at $z \sim 2$ (but see both papers for a discussion of uncertainties and assumptions).

Our completeness limit of $K_{\mathrm{AB}} = 22.9$ mag is roughly equal to the Reddy et al. (2005) DRG depth over a similar redshift range, and we find the same SFRD for DRGs of ~0.02 $M_\odot$ yr^{-1} Mpc^{-3}; thus, the X-ray and MIR-determined SFRD measurements agree that the DRGs produce roughly 20% of the total SFRD of optical and NIR-selected star-forming galaxies. A consistent picture is seen at longer wavelengths. If we use the 24 μm flux density of each DRG to predict its approximate 850 μm flux density, we find that our SFRD estimate is dominated by objects with $S_{850\,\mu\mathrm{m}} > 1$ mJy, and thus again DRGs produce ~20% of the total SFRD as measured at submillimeter wavelengths. In conclusion, DRGs, to a depth of $K_{\mathrm{AB}} = 22.9$ mag, are important contributors to the total SFRD at $z \sim 2$ and, by extension, to the assembly of massive galaxies.

6. SUMMARY

The analysis presented here indicates that DRGs constitute a heterogeneous population, with the majority consisting of luminous and dusty starburst galaxies. We find that >65% of the EHDF-S sample are such systems, and this is in good agreement with similar *Spitzer* studies (Papovich et al. 2006) and rest-frame optical SED modeling (Förster Schreiber et al. 2004; Labbé et al. 2005). Using the 24 μm flux, we estimate an average SFR for the population (to $K_{\mathrm{AB}} = 23.2$) of $130 \pm 30\ M_\odot$ yr^{-1}, in line with earlier estimates from optical, submillimeter, and X-ray studies. Normalizing the SFR to the rest-frame L_V yields $\mathrm{SFR}/L_V \sim 19\ M_\odot\ \mathrm{yr}^{-1}(L_\odot \times 10^{-10})^{-1}$ but with substantial scatter around this value. The scatter cannot be explained solely by redshift uncertainties and indicates a real difference in the individual properties' DRGs. Overall, DRGs are important contributors to the SFRD at $z \sim 2$ at a level of 0.02 $M_\odot$ yr^{-1} Mpc^{-3} to our 100% completeness limit of $K_{\mathrm{AB}} = 22.9$.

Research by T. M. A. W. is supported by a VENI Research Fellowship, through the Nederlanse Organisatie voor Wetenschappelijk Onderzoek. D. M. is supported by NASA LTSA NNG04GE12G. We are grateful to N. M. Förster Schreiber for a careful reading and insightful comments on an early version of this work.

REFERENCES

Chapman, S. C., Blain, A. W., Smail, I., & Ivison, R. J. 2005, ApJ, 622, 772
Coleman, G. D., Wu, C.-C., & Weedman, D. W. 1980, ApJS, 43, 393
Condon, J. J. 1992, ARA&A, 30, 575
Egami, E., et al. 2004, ApJS, 154, 130
Elbaz, D., Cesarsky, C. J., Chanial, P., Aussel, H., Franceschini, A., Fadda, D., & Chary, R. R. 2002, A&A, 384, 848
Engelbracht, C. W., Gordon, K. D., Rieke, G. H., Werner, M. W., Dale, D. A., & Latter, W. B. 2005, ApJ, 628, L29
Förster Schreiber, N. M., et al. 2004, ApJ, 616, 40
Franx, M., et al. 2003, ApJ, 587, L79
Garrett, M. A. 2001, in ASP Conf Ser. 249, The Central Kiloparsec of Starbursts and AGN, ed. J. H. Knapen, J. E. Beckman et al. (San Francisco: ASP), 652
Gawiser, E., et al. 2006, ApJS, in press (astro-ph/0509202)
Genzel, R., & Cesarsky, C. J. 2000, ARA&A, 38, 761
Gordon, K. D., et al. 2005, PASP, 117, 503
Hogg, D. W., Tremonti, C. A., Blanton, M. R., Finkbeiner, D. P., Padmanabhan, N., Quintero, A. D., Schlegel, D. J., & Wherry, N. 2005, ApJ, 624, 162
Huang, J.-S., et al. 2004, ApJS, 154, 44
———. 2005, ApJ, 634, 137
Huynh, M., Jackson, C. A., Norris, R., & Prandoni, I. 2005, AJ, 130, 1373
Ivison, R. J., et al. 2004, ApJS, 154, 124
Kennicutt, R. C., Jr. 1998, ApJ, 498, 541
Knudsen, K. K., et al. 2005, ApJ, 632, L9
Labbé, I., et al. 2005, ApJ, 624, L81
Papovich, C., et al. 2004, ApJS, 154, 70
———. 2006, ApJ, in press
Reddy, N. A., Erb, D. K., Steidel, C. C., Shapley, A. E., Adelberger, K. L., & Pettini, M. 2005, ApJ, 633, 748
Richards, E. A. 2000, ApJ, 533, 611
Rigby, J. R., et al. 2005, ApJ, 627, 134
Rubin, K. H. R., van Dokkum, P. G., Coppi, P., Johnson, O., Förster Schreiber, N. L., Franx, M., & van der Werf, P. 2004, ApJ, 613, L5
Rudnick, G., et al. 2001, AJ, 122, 2205
———. 2003, ApJ, 599, 847
Shapley, A. E., et al. 2001, ApJ, 562, 95
Steidel, C. C., Adelberger, K. L., Giavalisco, M., Dickinson, M., & Pettini, M. 1999, ApJ, 519, 1
Stetson, P. B. 1987, PASP, 99, 191
van Dokkum, P. G., et al. 2003, ApJ, 587, L83
Wu, H., et al. 2005, ApJ, 632, L79